Diagnostics Beamline Development

(Sector 35)

Bingxin Yang and Alex H. Lumpkin

The missions of the APS diagnostics beamlines are:

(1) To support user operations by providing on-line information about the electron beam on a 24-hour basis;

(2) To support machine physics studies by providing photon diagnostics on beam properties, transverse and longitudinal;

(3) To conduct research and development of diagnostics for future light sources.

Strategies:

Utilize and develop time-resolved imaging with optical and x-ray synchrotron radiation to support the mission.

OUTLINE

I. Overview of Sector 35

II. Beam Quality Assurance for User Operations

(A)   Pinhole camera upgrade: beam position, size, and emittance data tracking

(B)   Bunch purity and bunch cleaning

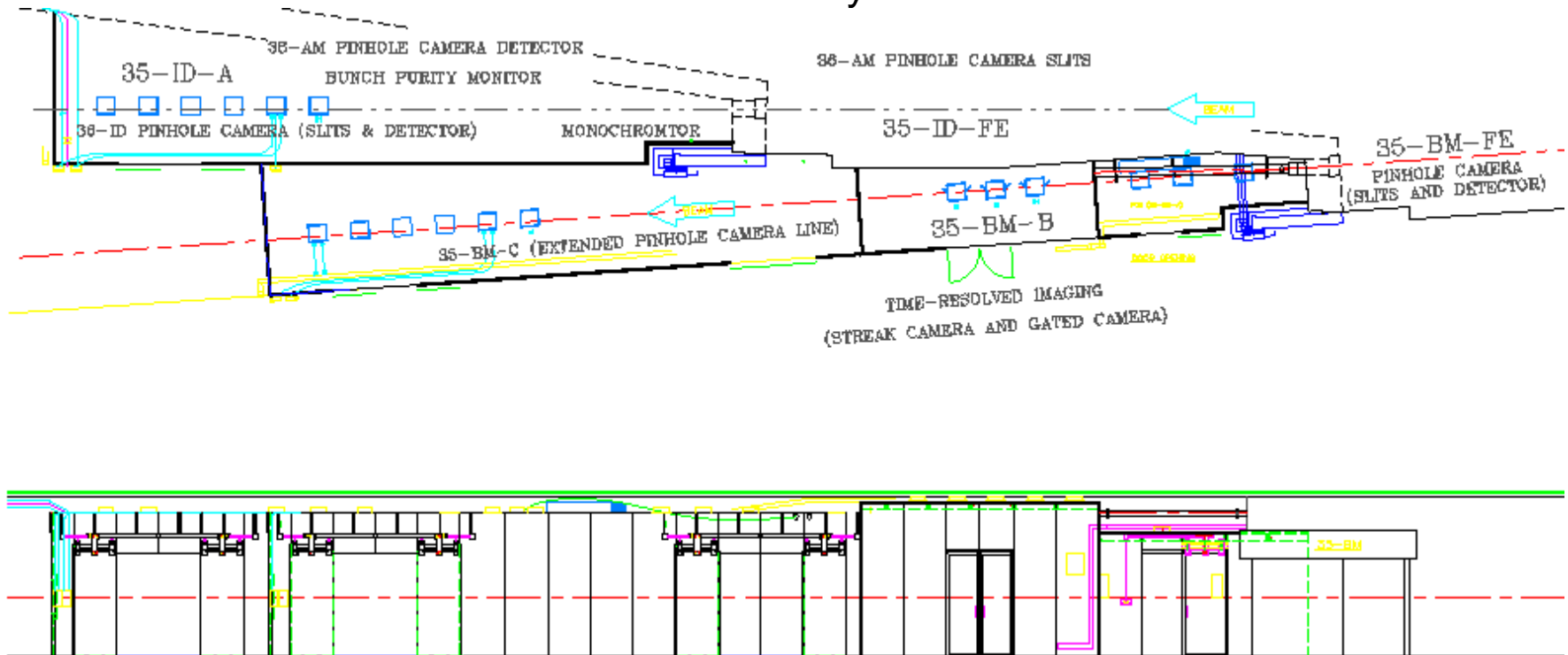## III. Undulator-Based Electron Beam Measurements

(A)   Emittance measurements

(B)   Relative beam energy measurement

(C)   Energy-dependent e-beam property measurements

(D)   Observation of lowest effective emittance in APS-SR straight sections: 3.5 nm rad

IV. Summary and Future Developments

I. Overview of Sector 35

Sector 35 Layout

Three beamlines:

35-BM: X-ray pinhole camera, time-resolved imaging (visible light)
35-ID: Undulator-based diagnostics
36-AM: Pinhole camera at low-dispersion source, bunch purity monitor

ADVANCED PHOTON SOURCE

SECTOR 35 IMPORTANT EVENTS

- Visible light CCD camera   3/18/95
  Image of the first APS SR beam

- X-ray pinhole camera (BM: high dispersion point)   3/96
  Pinhole in air, detector in tunnel, M = 0.44

- X-ray pinhole camera (BM)   4/97
  Pinhole in vacuum, detector in tunnel, M = 1.06

- ID beam divergence measurement   5/2/98
  Monochromator in air, distance @ 28.4 m, 36.5 m

- X-ray pinhole camera (AM: low dispersion point)   6/98
  Pinhole in vacuum, detector in hutch, M = 1.55

- X-ray streak camera first image (AM)   11/97

- BM pinhole camera improvement   5/98-1/99
  Upgrade in-tunnel detector, stabilize water temperature,
  improved video processing

- Second video frame grabber implemented   8/98
  Mobile MV-200 used at Sector 35

- ID horizontal beam size measurement   8/99
  Pinhole slits after monochromator, M = 0.277

- ID beam divergence measurement   9/98
  Monochromator in vacuum @28.4m

- Simultaneous tracking of beam size and divergence   1/99
  35-ID beamline

- ID-based e-beam measurements   1999
  Beam energy spread, energy-dependent properties,
 low emittance to 3.5 nm·rad

II. Beam Quality Assurance for User Operations

(A) Beam position, size and emittance: pinhole camera upgrade and data tracking

The pinhole camera at 35-BM continued to be our workhorse in 1998-1999. Upgrades performed during 1998 - 1999:

- Stabilizing cooling water temperature to $\pm 0.1°F$ (ASD/MEC)

- Installing new imaging detector (better optics, 80 µm thick scintillator)

- Improving video signal processing

Data quality has been significantly improved. At 1-Hz bandwidth, we have better than 1-µm stability in measured beam size, as shown by the following data set.
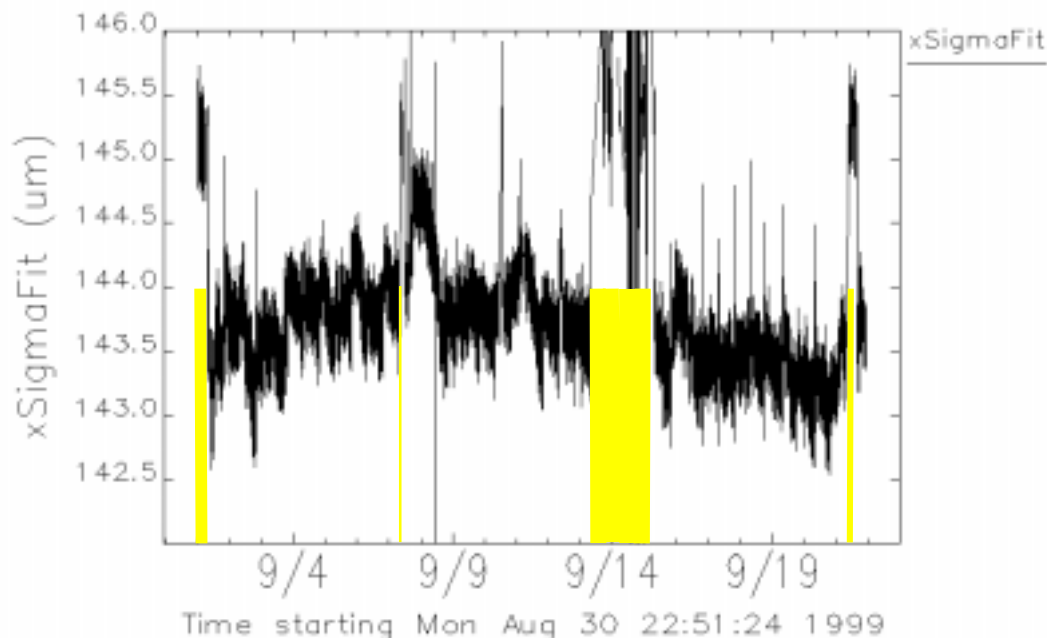

The rms horizontal beam size during the current month recorded by the APS data logger: Significant variations can be seen during machine studies on September 1, 7, 14-15, and 21.

ADVANCED PHOTON SOURCE

Insertion device gap changes have strong effect

During user runs, the beam size can vary up to 2.5 µm, largely due to ID gap changes by the user. The following data (2-week and 2-day tracking) show strong (anti)correlation of total energy loss by the APS insertion devices with emittance.
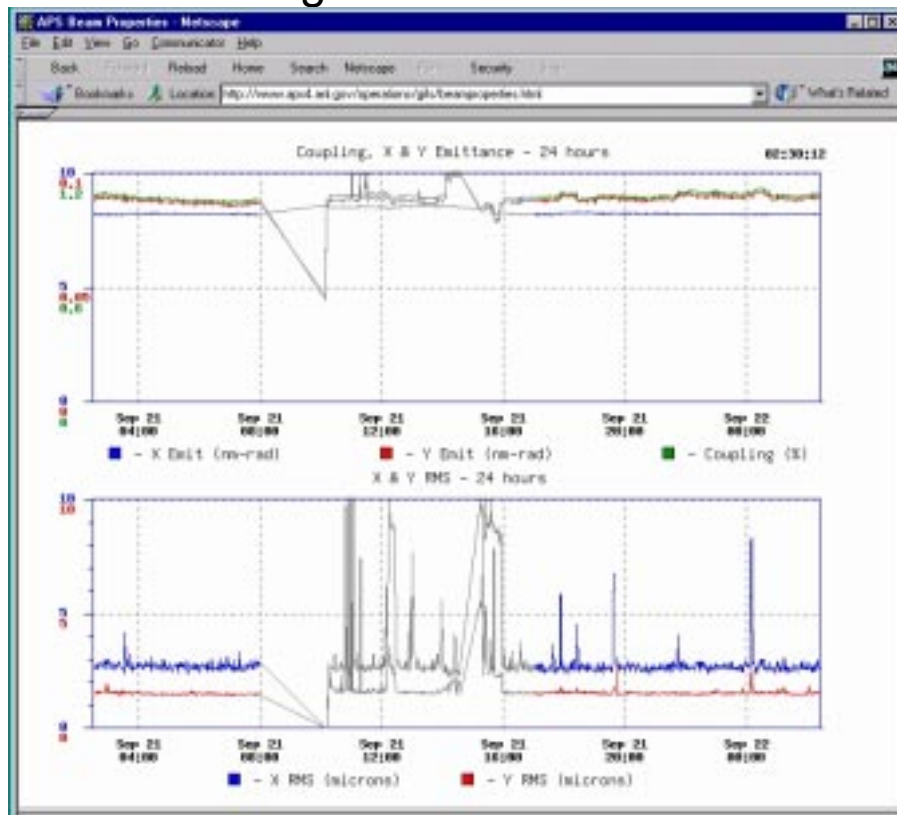

Time starting Wed Sep 1 21:36:16 1999
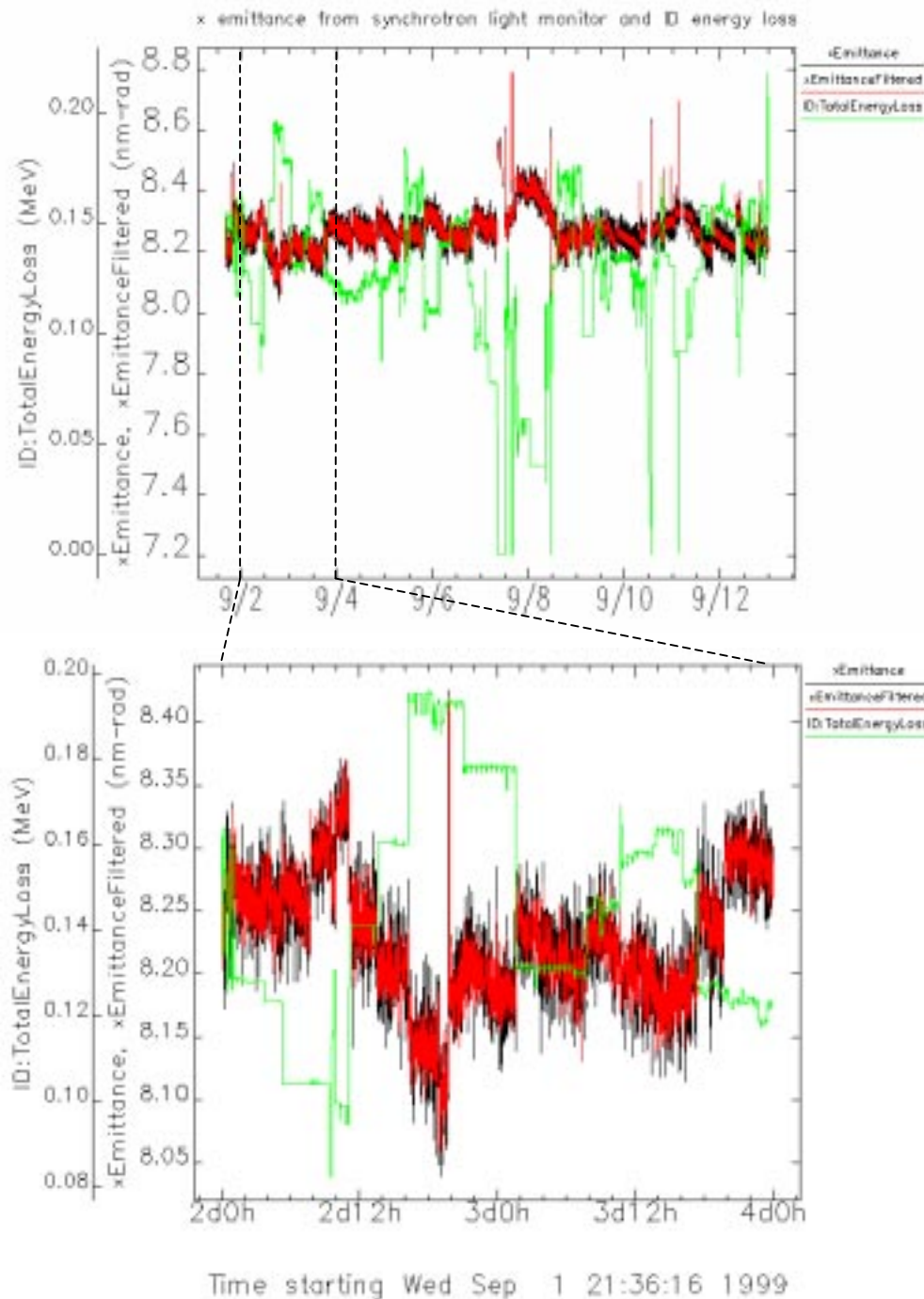
ADVANCED PHOTON SOURCE

The beam position, size, and emittance data are available to the Operations Group through EPICS (1 update / sec.)
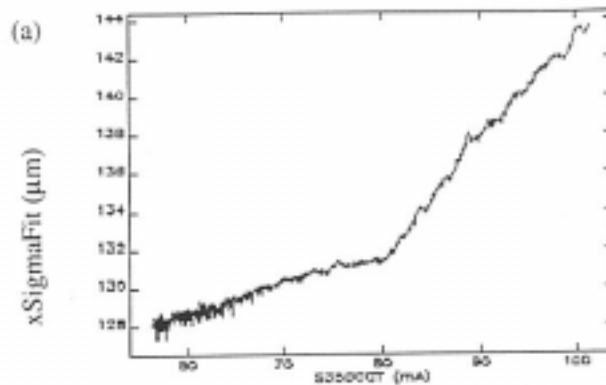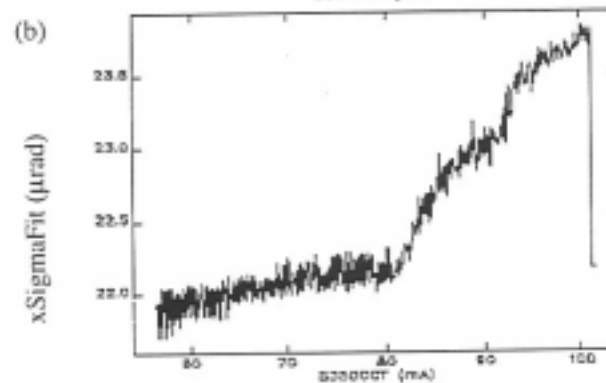

and to the users through the Web

Diagnose subtle beam instabilities

Having a stable measurement of beam size helped identify a subtle transverse beam instability (> 85 mA) and a longitudinal beam instability (> 101 mA) during user runs in 1998. The instabilities were suppressed. (Lumpkin et al. PAC99)
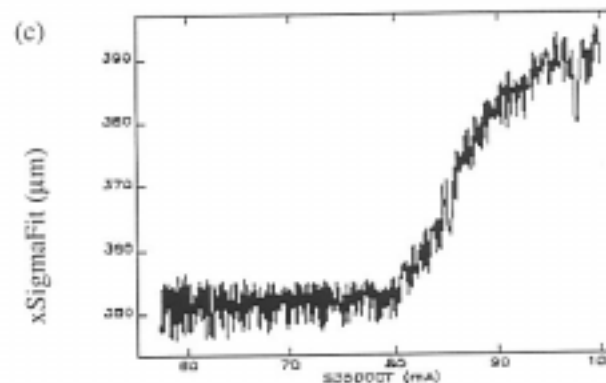
35-BM source size
(horizontal)

35-ID divergence
(horizontal)

35-ID source size
(horizontal)

Resolution measurement of pinhole camera

The measured vertical beam size was assumed to be the quadrature sum of the camera resolution and the true beam size

$$\sigma_{\exp}{}^2 = \sigma_R{}^2 + \sigma_y{}^2.$$

For a single bunch fill, the beam lifetime is dominated by Touschek scattering (A. Ropert, LS-275), which is proportional to the bunch volume. Fitting the measured vertical beam sizes and lifetime to the simple function gives:

Pinhole camera resolution = 22 μm

Vertical beam size = 16 μm (smallest observed)

Skew Quad Scan for 35-BM Pinhole
Camera Resolution Measurement
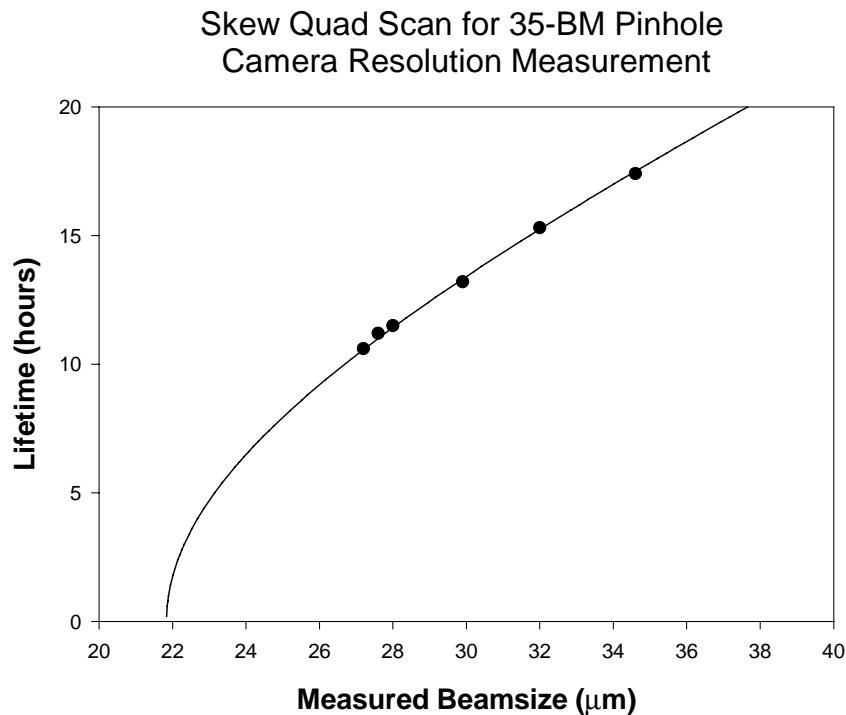
0.2% vertical coupling is the lowest observed to date.

Summary for pinhole camera upgrade
beam position, size and emittance data tracking

- In FY1999, the performance of the 35-BM x-ray pinhole camera has reached a submicron level of stability in transverse beam size measurements due to hardware and software upgrades.

- The deduced emittance data is now available to the users through the Web (ASD/OPS).

- During user operations, the APS storage ring horizontal beam size at the BM is normally stable within a 2-µm range (1.4% @ BM, ~3% @ ID). Most variations of horizontal beam size and emittance are induced by insertion device gap changes.

- In at least two incidences, the x-ray pinhole camera has enabled the identification and correction of subtle beam instabilities before users realized their existence.

- The camera resolution has reached 22 µm in mid-1999. It was used to directly observe a vertical coupling of 0.2%, the lowest on the APS storage ring so far.

Further upgrades
(needed for operations with 0.1% coupling, σ_y = 10 µm)

- The extension of the pinhole camera beamline is in progress. It is expected to improve resolution to the level of 10 - 15 µm.

- Approaches for further improvement in resolution to the level of 5 - 10 µm are being studied.

- Improvement of the stability of transverse size measurement to < 0.5 µm level (1 Hz bandwidth) will be pursued in FY2000.

(B) Bunch purity and bunch cleaning

A bunch-purity monitor was implemented by cloning the system in Sector 3 (E. Alp)
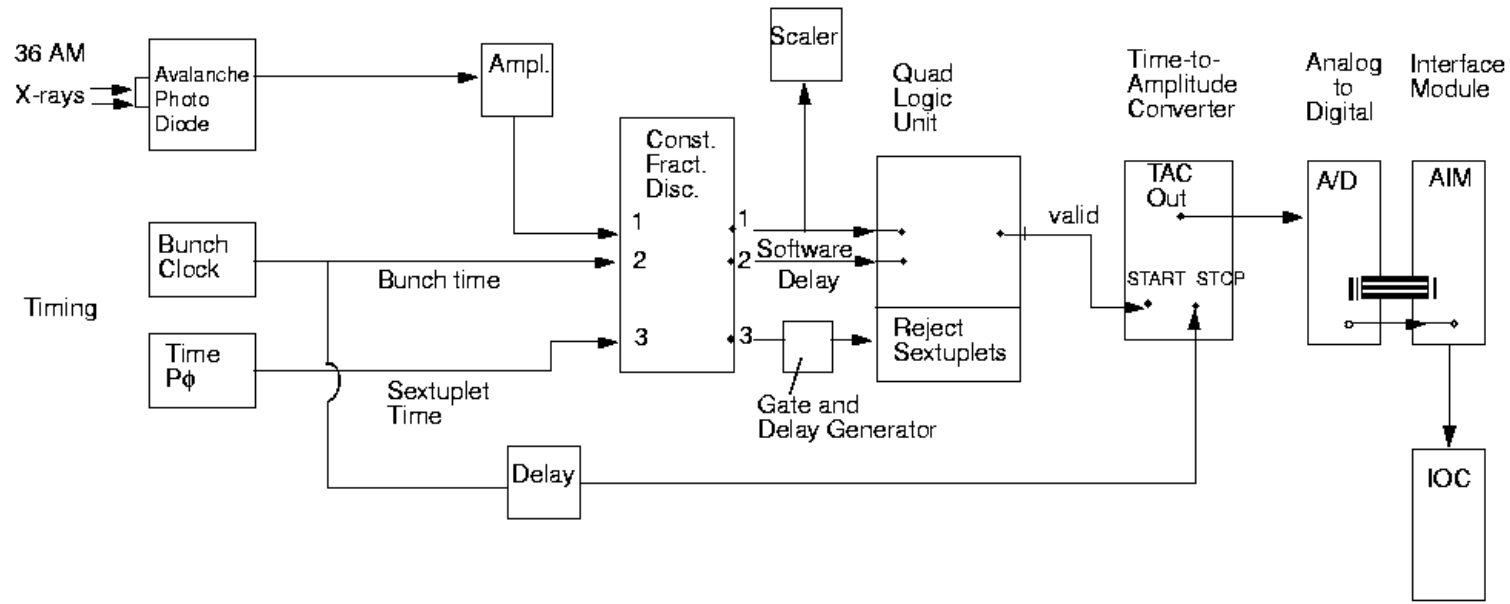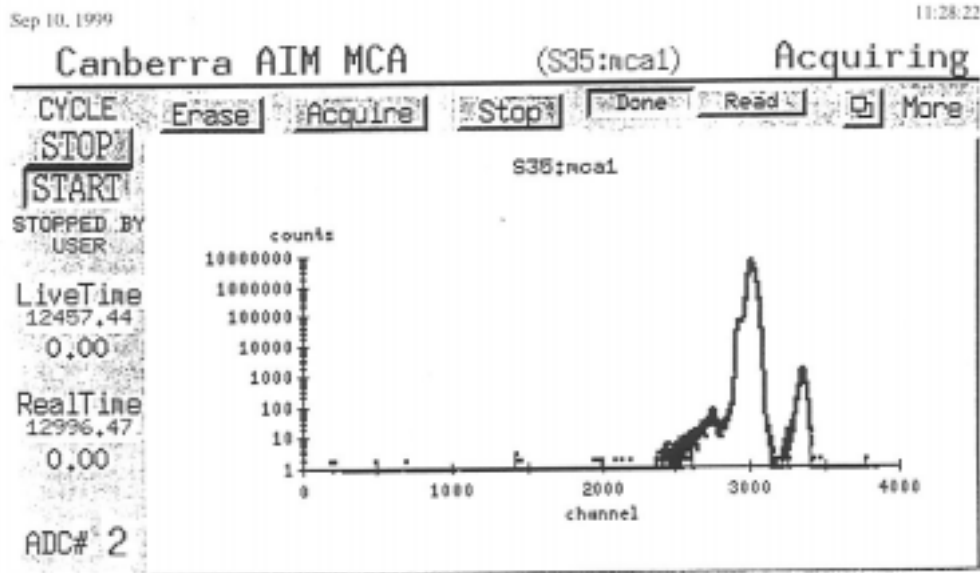

Schematic of Sector 35 bunch purity monitor

(The APD is located in 35-ID-A station, taking x-rays from 36-AM pinhole line)

ADVANCED PHOTON SOURCE

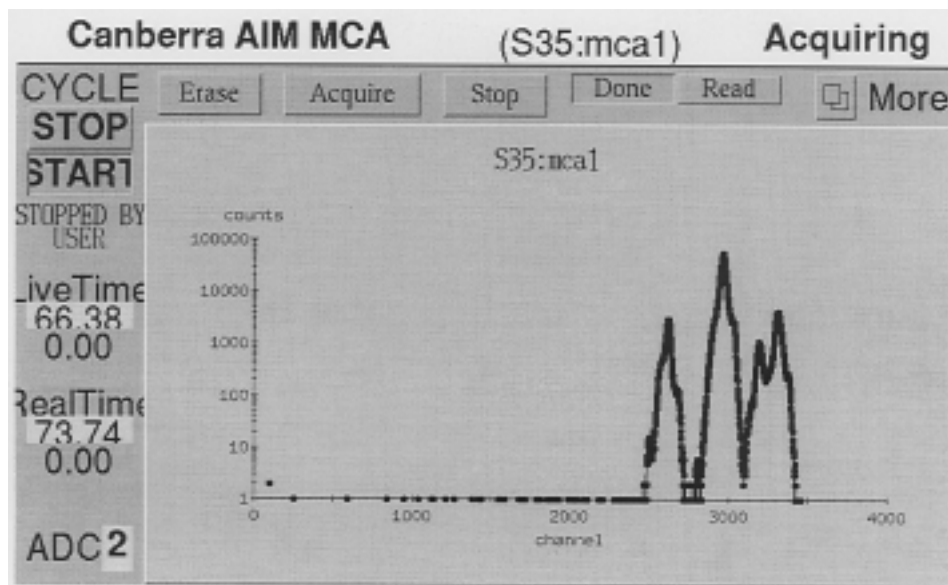During user operation, bunch-purity is routinely checked after each fill

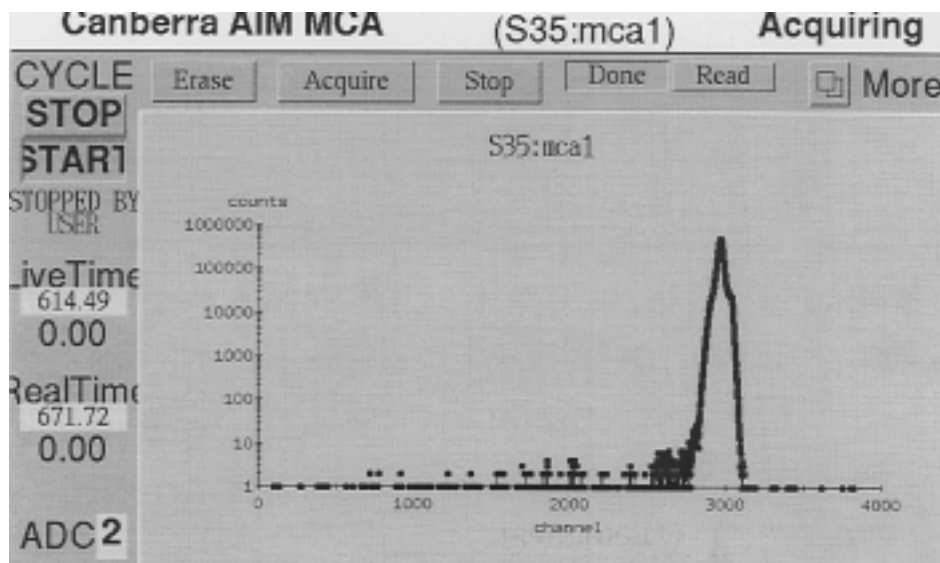Control screen for the bunch-purity monitor

ADVANCED PHOTON SOURCE

Support bunch-cleaning experiments

The bunch-purity monitor was also used to support bunch-cleaning experiments, an effort towards eventual injections without the Positron Accumulator Ring.

Charge distribution before bunch cleaning

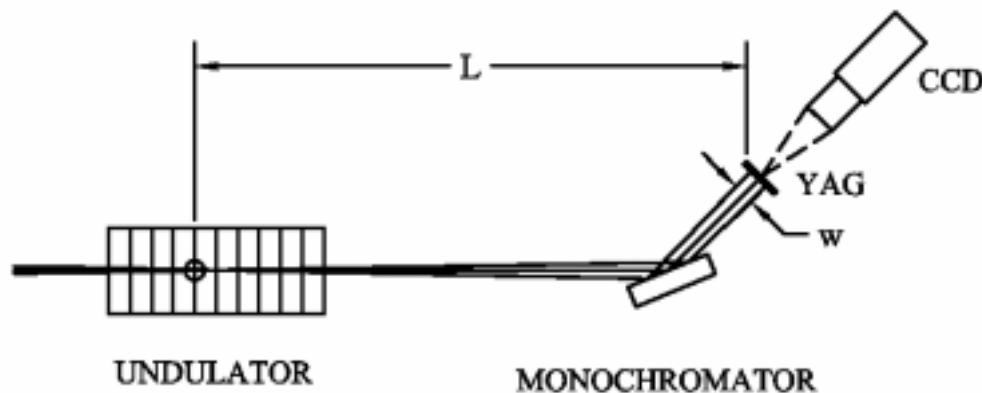Charge distribution after bunch cleaning

III. Undulator-based Electron Beam Measurements

(A) Emittance measurement with undulators

Introduction (a simplified picture)

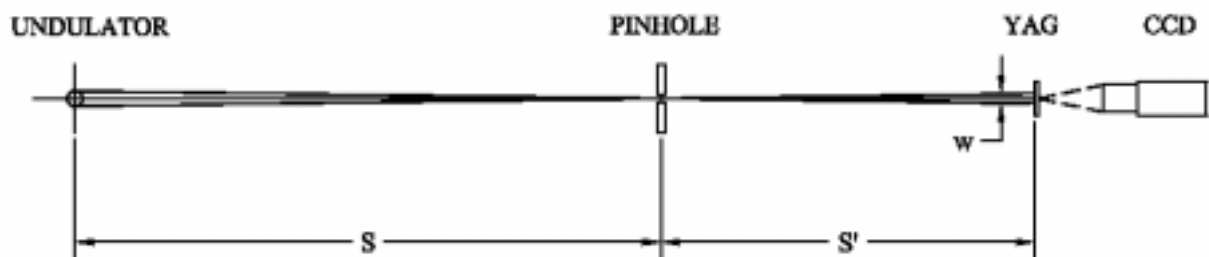1. Divergence measurement with monochromatic undulator beam

Monochromator select photon energy: $\omega < \omega_1$

Beam Divergence $= w / L$

2. Pinhole camera for source size measurement

Source size $= w * S / S'$

Twiss parameters and systematic errors (geometrical optics approximation)

X-ray beam cross section

X-ray image size

S_m

Z

S

S'

Pinhole or lens aperture

Electron Beam waist location: $Z = \alpha / \gamma$

- Apparent divergence is larger due to the contribution of e-beam size
- Apparent source size is smaller due to the directional nature of undulator radiation

ADVANCED PHOTON SOURCE

Twiss parameters and systematic errors (geometrical optics approximation)

Effective divergence from x-ray beam cross section ($Z = \alpha / \beta$)

$$S_m{}^2 \sigma_{x',eff}{}^2 = (S_m - Z)^2 \sigma_{x'}{}^2 + S_m{}^2 \sigma_m{}^2 + \sigma_{x0}{}^2$$

Effective beam size from pinhole camera (or any small aperture optic)

$$\sigma_{x,eff}{}^2 = \frac{S^2 \left(\sigma_{x'0}{}^2 + \sigma_\gamma^2 + \dfrac{Z^2}{\beta_0{}^2} \sigma_\gamma^2 \right)}{\sigma_{x'0}{}^2 (S - Z)^2 + \sigma_\gamma^2 S^2 + \sigma_{x0}{}^2} \, \sigma_{x0}{}^2$$

Product of the two effective measurements

$$\varepsilon_{x,eff} = \sigma_{x,eff} \sigma_{x',eff} = \frac{\varepsilon}{R}$$

with correction factor

$$\frac{1}{R} = \frac{S}{S_m} \sqrt{ \frac{\beta_0{}^2 + (S_m - Z)^2 + S_m{}^2 \dfrac{\sigma_m{}^2}{\sigma_{x'}{}^2}}{\beta_0{}^2 + (S - Z)^2 + S^2 \dfrac{\sigma_\gamma^2}{\sigma_{x'}^2}} \cdot \left(1 + \frac{\beta \sigma_\gamma^2}{\beta_0 \sigma_{x'}^2} \right) },$$

a slow function of Twiss parameters. The systematic effects are nearly completely cancelled for $S \approx S_m$.

More complications: Fresnel diffraction
point spread function of pinhole camera

A pinhole camera point spread function (PSF) is best modeled by broadband Fresnel diffraction pattern.

$$f_5(\tilde{x}) = \frac{1}{2\pi\sqrt{N}} \int_0^2 \frac{dt}{\eta t} \left\{ e^{-\frac{\tilde{\varphi}_0^2\tilde{\sigma}_0^2 + \alpha^2(\psi_0+\tilde{\varphi}_0\tilde{x})^2}{2\eta^2}} \sin\frac{\psi_0+\tilde{\varphi}_0\tilde{x}}{\eta^2} + (\tilde{x}\to-\tilde{x}) \right\}$$
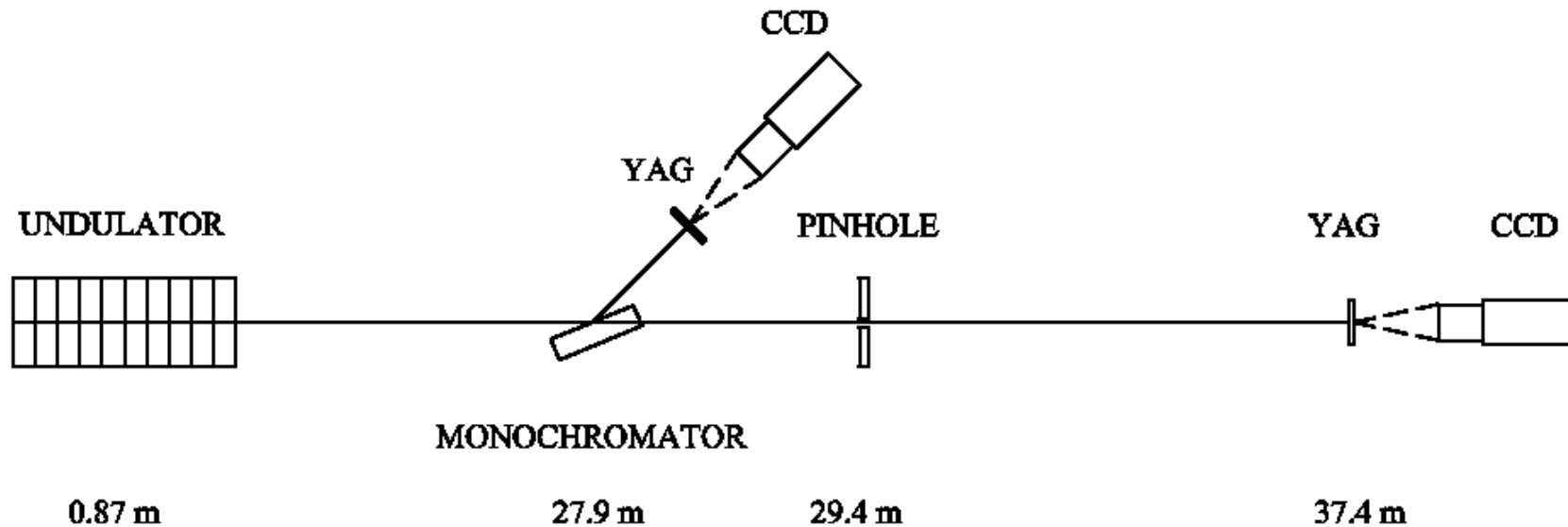
The observed pinhole data display strong Fresnel diffraction signatures.

**INTEGRATED VERTICAL INTENSITY PROFILE
SHOWS FRESNEL DIFFRACTION SIGNATURE**

Gaussian

Hybrid = Geometrical + Fraunhofer

Fresnel
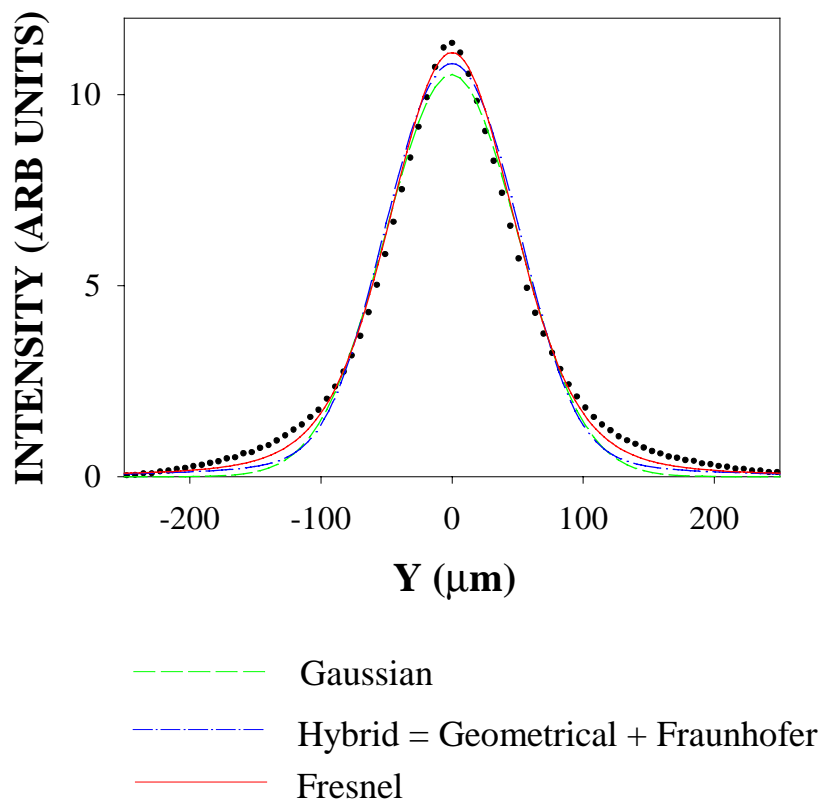
EXPERIMENTAL SET UP

Emittance correction factor, $R \approx 0.92$

The **APS Diagnostics Undulator** is optimized for beam diagnostics

- Short period: 1.8 cm $\times$ 198 period
- Low power : 25.9 keV @ 30 mm gap, < 1 W x-ray power
- Low divergence : 2.6 µrad
- Low field error: rms slope error < 1 µrad

ADVANCED PHOTON SOURCE

Monochromator optimized for divergence measurement

- Direct imaging of unmasked undulator beam: Interpretation straightforward
- Single crystal monochromator: Avoid artifacts associated with double crystal monos
- Short distance (0.5 m) from crystal to scintillator screen: Minimize effect of heat-induced crystal distortion
- Thin silicon crystal (0.3 mm) can be used in Bragg (400) or Laue (220) reflection: Allow substantial hard x-ray flux to pass for source size measurement. In vacuum chamber with 1-mm Be window, located @ 27 m from ID
- Detector: YAG crystal 0.5 mm thick + 7:5 optics + CCD camera, located @ 27.5 m

Pinhole camera parameters (M = 0.32)

- Pinhole slits: water cooled 6-mm tungsten blades, located @ 28.5 m, 25 μm × 25 μm
- Detector: YAG crystal (0.17 mm) + Navitar zoom lens + SONY CCD camera @ 37.4 m

A typical undulator-based emittance measurement

User run (9/22/99 4:00 AM)

Horizontal emittance = 353 μm × 26.8 μrad × 0.92 = 8.7 nm·rad

(Emittance deduced from 35-BM pinhole camera results is 8.17 nm·rad at the time)

Summary for emittance measurement with undulators

- Undulator beam contains information about divergence and size of the electron beam. It offers the potential of measuring e-beam emittance without relying on knowledge of beta functions.

- Quantitative analysis shows that it is not trivial to extract emittance information from undulator measurements. Two measurements are not enough to achieve total independence from the knowledge of lattice functions (Twiss parameters).

- We have implemented simultaneous measurement of beam "divergence" and "size" in Beamline 35-ID using a thin crystal monochromator and pinhole camera.

- Strong Fresnel diffraction characteristics have been observed in 35-ID pinhole images.

Instrument resolution compared to beam properties

| Quantity	Typical value	Resolution	Comment
Horizontal divergence	26 µrad	~2.6 µrad	Resolution correction not needed
Horizontal source size	340 µm	~40 µm	Resolution correction not needed
Vertical divergence	5 µrad	~2.6 µrad	Some resolution correction
Vertical source size	20 µm	~40 µm	Resolution limited

- Improvement of vertical resolution (with imaging x-ray optics) is clearly needed.

- A third screen is also desirable in deducing emittance without relying on knowledge of Twiss parameters.

(B) Relative beam energy measurements with undulators

ANGLE-INTEGRATED FLUX (N=198)
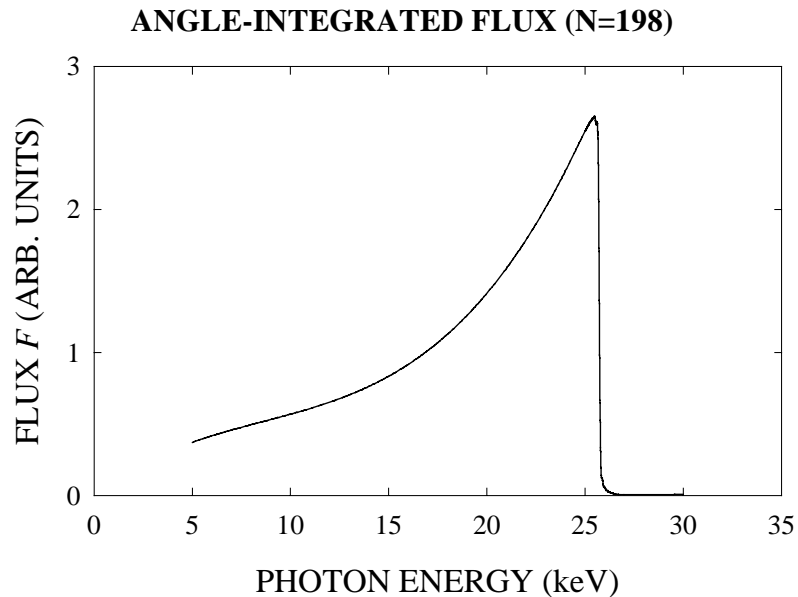
Take derivative of the spectrum near the resonance, and plot against $\Delta\omega/\omega$. The result is a sharp peak centered at the nominal harmonic energy. Its FWHM is ~1/nN (n = harmonic #, N = # of periods). The following example is calculated for the APS Diagnostics Undulator (fundamental).

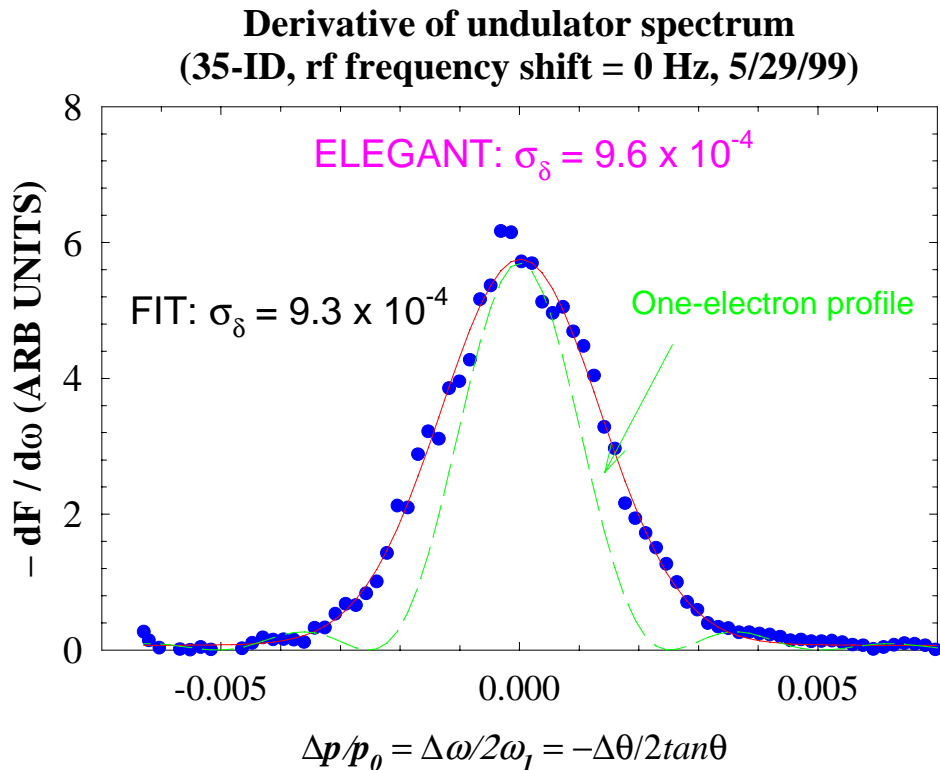**DERIVATIVE OF INTEGRATED SPECTRUM**

$$\sigma \sim 0.4/N$$

$$\Delta\omega/\omega = 2\,\Delta p/p$$
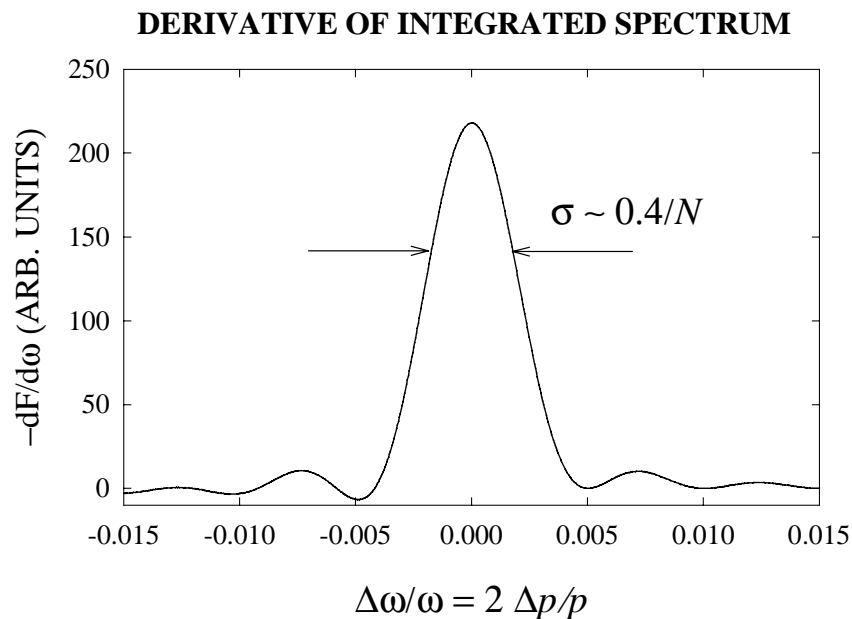
Electron Beam Energy Measurement Data

1. Scan monochromator θ-2θ, record angle-integrated spectrum.

2. Convert the change of photon energy ω to electron energy change:
$$\frac{\Delta p}{p_0} = \frac{\Delta\omega}{2\omega_1} = -\frac{\Delta\theta}{2\tan\theta_1}$$

3. Fit the derivative of the spectrum with the convolution of Gaussian and SINC function and obtain the energy centroid (relative) and energy spread.

Derivative of undulator spectrum
(35-ID, rf frequency shift = 0 Hz, 5/29/99)

ELEGANT: $\sigma_\delta = 9.6 \times 10^{-4}$

FIT: $\sigma_\delta = 9.3 \times 10^{-4}$

One-electron profile

$-$ dF / dω (ARB UNITS)

$\Delta p/p_0 = \Delta\omega/2\omega_1 = -\Delta\theta/2\tan\theta$

Advantages of using the undulator angle-integrated spectrum

- **Clean**: independent of beam emittance and lattice functions.
- **Accurate:** only monochromator angle needs good calibration.
- **Simple** data collection and treatment.
- **Efficient**: do not lose photons in apertures, good S/N ratio.

ADVANCED PHOTON SOURCE

(C) Energy-dependent beam property measurements

Electron beam**:** User fill, 100 mA in 6+25*3 bunches

Experimental Approach**:** Scan storage ring rf frequency (electron energy), and record

- BM and ID pinhole camera image size and centroid
- ID monochromator beam image size and centroid
- ID angle-integrated photon flux with monochromator scan
- Transient images with BM gated camera on kicker excited beam

Physical quantities extracted from the data

- Electron energy as a function of rf frequency shift → **momentum compaction factor** *
- Beam centroid as a function of beam energy → **dispersion** (x & y)
- Beam direction as a function of beam energy → **dispersion slope** (x & y)
- **Horizontal emittance** as a function of energy *
- Longitudinal emittance as a function of energy: **energy spread***
- Longitudinal emittance as a function of energy: **bunch length** (planned)
- **Transverse damping*** as a function of energy (gated camera)
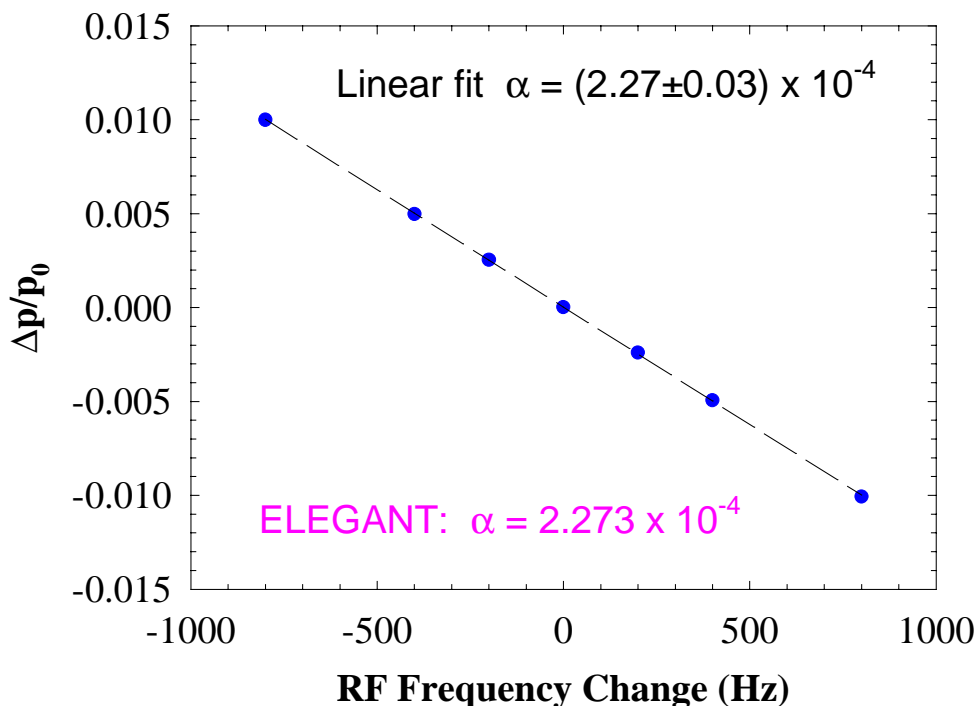- **Vertical emittance** as a function of energy (divergence only)

Momentum Compaction Factor Measurement

- At each rf frequency shift setting

  1. Scan monochromator θ-2θ, record angle-integrated spectrum.

  2. Fit the derivative of the spectrum with a Gaussian function. The centroid energy is the undulator ω_1 and proportional to γ^2.

  3. Convert the change of undulator energy ω_1 to electron energy change: $\Delta\omega/\omega_1 = 2\Delta\gamma/\gamma$

- Fit the e-beam energy change against rf frequency change to a straight line and convert to momentum compaction factor:

$$\alpha = -\frac{\Delta f}{f_0}\bigg/\frac{\Delta p}{p_0} = -2\frac{\Delta f}{f_0}\bigg/\frac{\Delta\omega}{\omega_1} = \frac{2\tan\theta_0}{f_0}\frac{\Delta f}{\Delta\theta}$$

APS-SR Electron Energy Change with RF Frequency
**(35-ID Monoscan, 5/29/99)**

Linear fit $\alpha = (2.27\pm0.03) \times 10^{-4}$

ELEGANT: $\alpha = 2.273 \times 10^{-4}$

$\Delta p/p_0$ vs RF Frequency Change (Hz)

For measurements of momentum compaction factors, the undulator data is very clean. One only needs to calibrate f and θ.

Electron Beam Energy Spread Measurement

- At each rf frequency shift setting

  1. Scan monochromator θ-2θ, record angle-integrated spectrum.

  2. Convert the change of photon energy ω to electron energy change: $\Delta\omega/\omega_1 = 2\Delta\gamma/\gamma_0$

  3. Fit the derivative of the spectrum with the convolution of Gaussian and SINC function and obtain the energy spread.
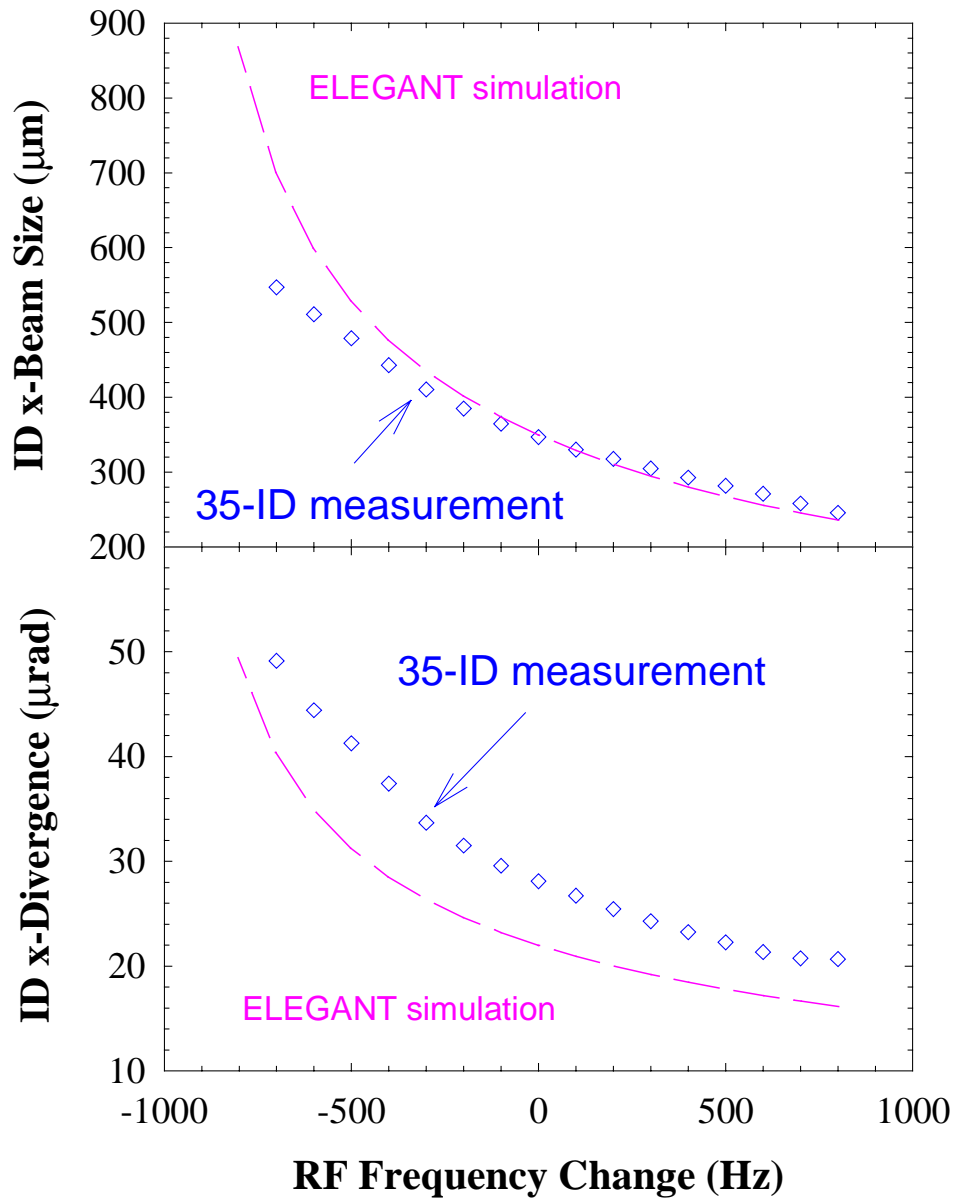
Storage Ring Energy Spread (5/29/99)
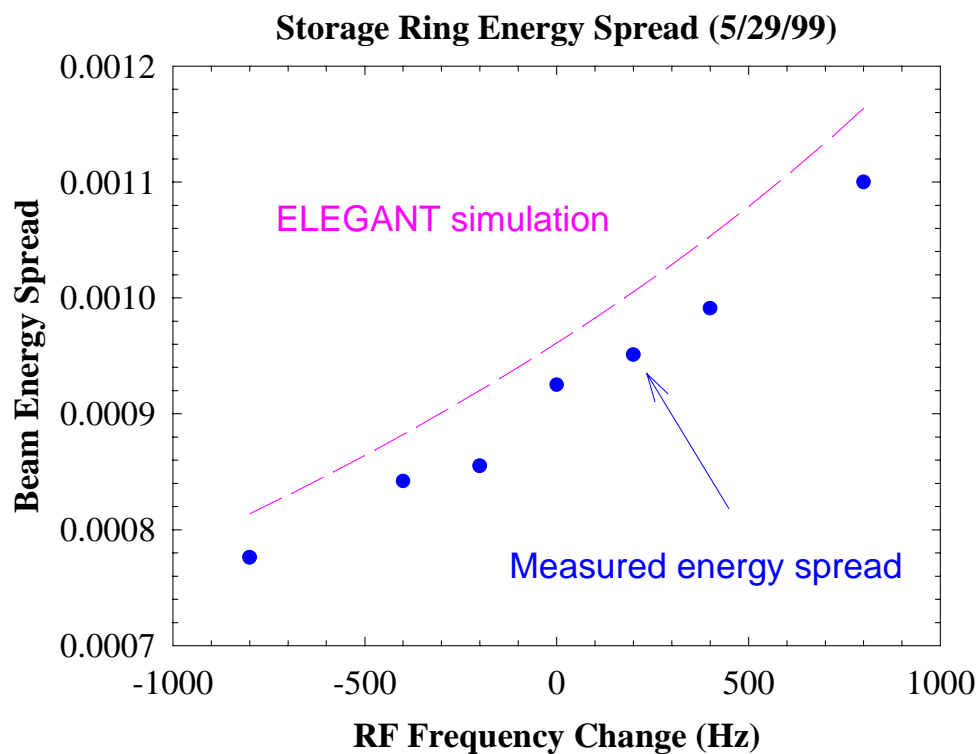
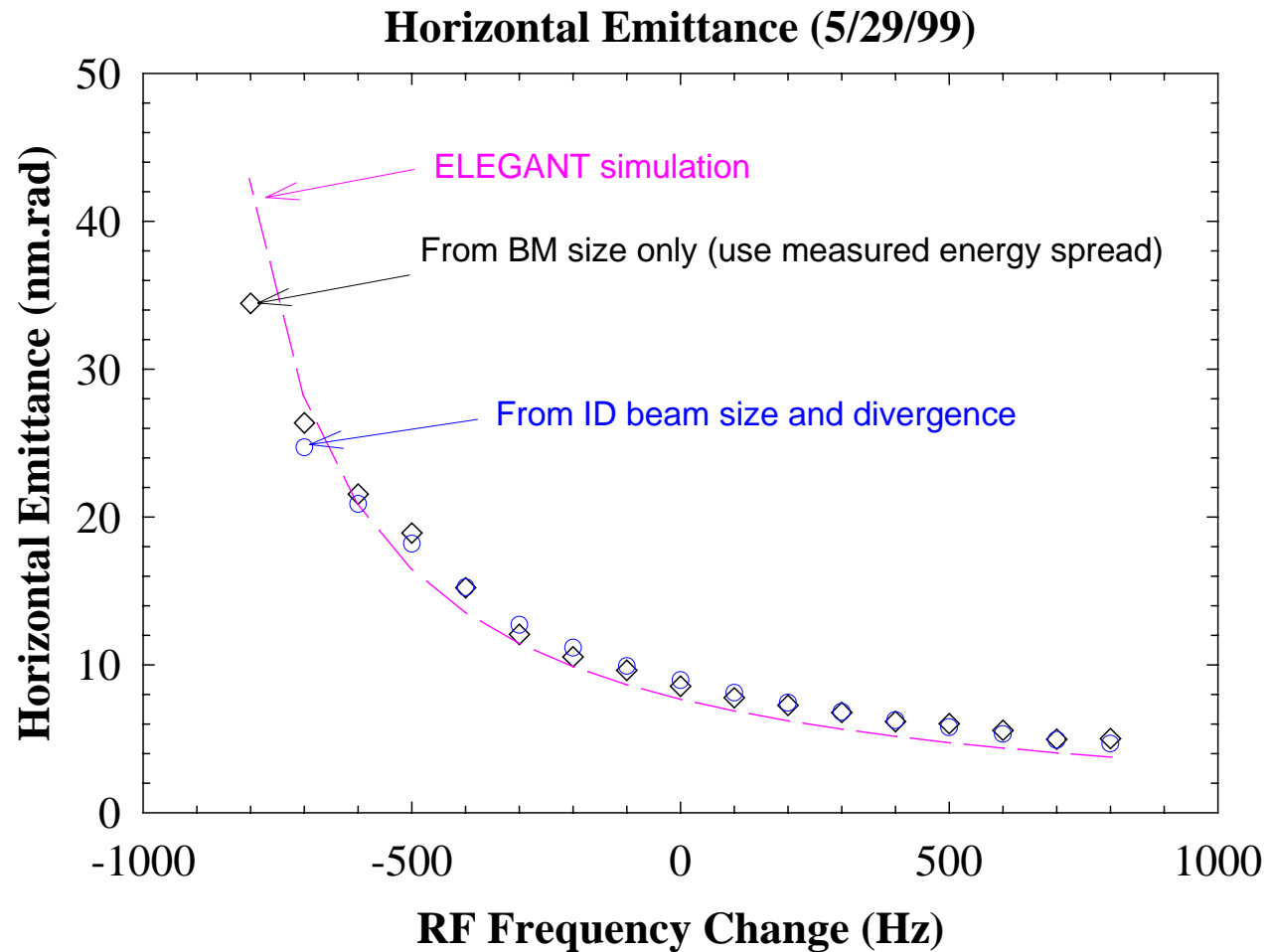Resolution of this technique is very good: Changes of energy spread under 10^{-4} can be clearly resolved!

Simultaneously Measured Divergence and Source Size

35-ID Emittance Measurement (Horizontal)
(5/29/99)

Comparison of ID and BM measurements
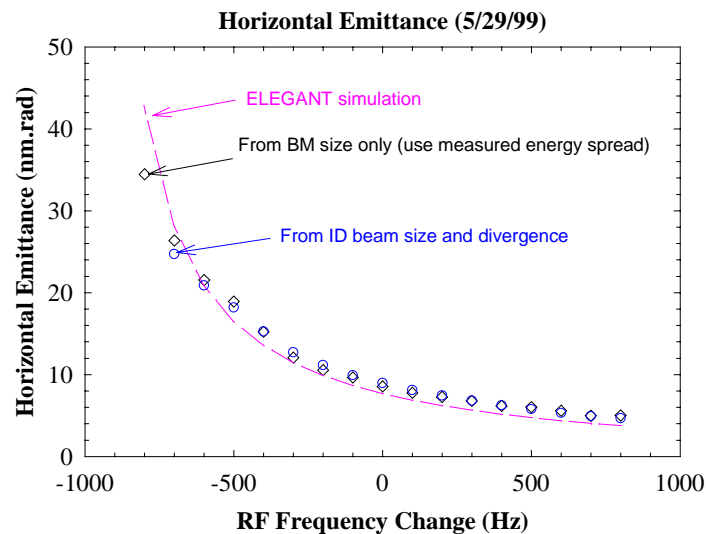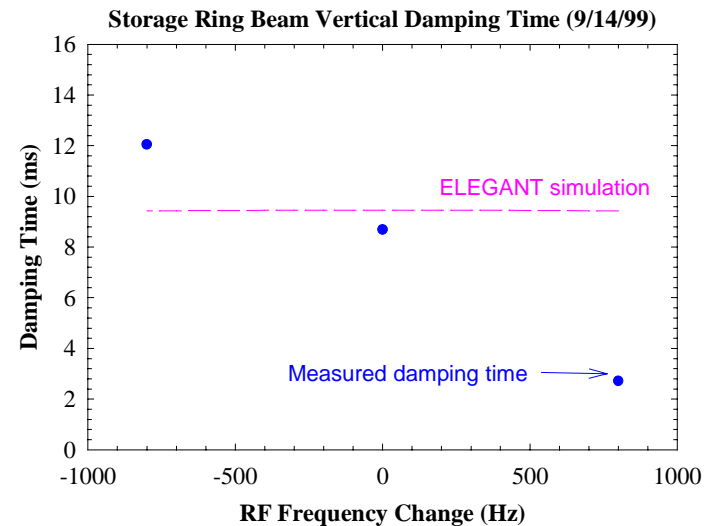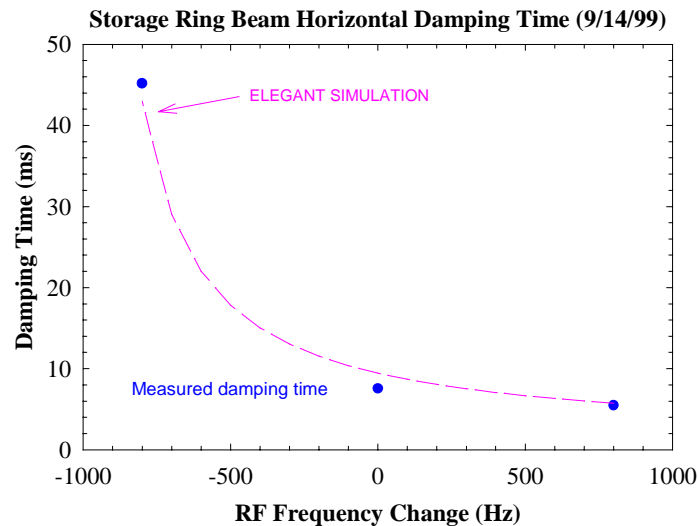
Horizontal Emittance (5/29/99)

It is important to apply the correct energy spread to BM source size to deduce emittance.

$$\varepsilon_x = \left\{\sigma_x{}^2 - \eta_x{}^2\sigma_\delta{}^2\right\}/\beta_x$$

Transverse Damping Time (gated camera measurements)

Storage Ring Beam Horizontal Damping Time (9/14/99)

ELEGANT SIMULATION

Measured damping time

Storage Ring Beam Vertical Damping Time (9/14/99)

ELEGANT simulation

Measured damping time

Horizontal Emittance (5/29/99)

ELEGANT simulation

From BM size only (use measured energy spread)

From ID beam size and divergence

The damping time measurements directly confirms the manipulation of the damping partition.

The shortened damping time (5.5 ms @ 800 Hz, 30% lower from 0 Hz) would further improve the performance of top-up operation if injection transient is present.

(D) Observation of the lowest effective emittance in APS ID @ 7 GeV

Two methods to reduce emittance

- **Introduce dispersion in straight section** (reduce quantum excitation, Ed Crosbie APS/IN/ACCPHY/95-1, and Louis Emery, 5/99).

  Dispersion contributes to beam size and divergence in straight section

$$\sigma_x^{\,2} = \beta_x \varepsilon_x + \left(\eta_x \frac{\sigma_E}{E} \right)^2, \text{ and } \sigma_{x'}^{\,2} = \gamma_x \varepsilon_x + \left(\eta'_x \frac{\sigma_E}{E} \right)^2$$

- **Manipulate damping partition to increase horizontal damping**
  The longitudinal and transverse damping rates obey the Robinson sum rules:

$$\frac{4}{\tau_\gamma} = \frac{1}{\tau_x} + \frac{1}{\tau_y} + \frac{1}{\tau_s} = \frac{1}{\tau_\gamma}\left(J_x + J_y + J_s \right)$$

  Changing partition ratio from 1:1:2 to 2:1:1 reduces horizontal emittance by half.

  - Changing rf frequency shifts the electron orbit in quadrupoles in the high dispersive sections, thus changing the partition number

  - Moving quadrupoles horizontally also changes the partition numbers

Applying rf frequency shift to the low-emittance lattice, we observed the lowest effective emittance in the APS storage ring to date.
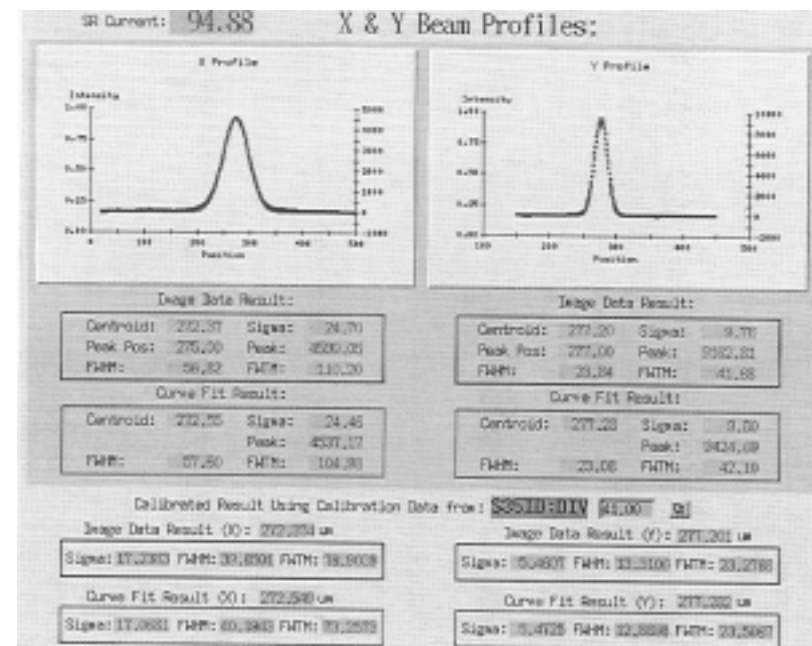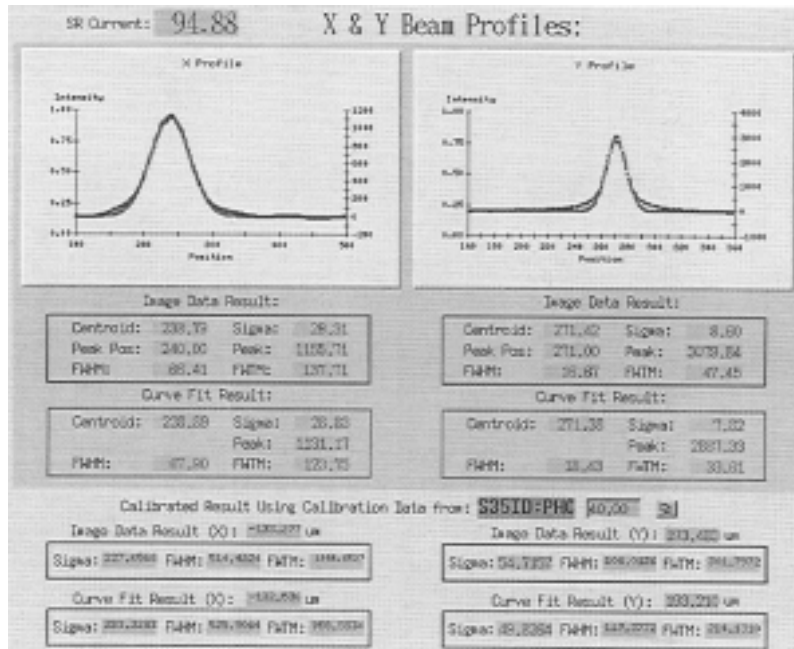
Observation of the lowest effective emittance in APS ID @ 7 GeV

Machine study run (5/29/99)
Dispersion in straight section (Crosbie-Emery low emittance lattice)
RF frequency shift +800 Hz (~3 mm orbit shift in high dispersion straight)

Effective horizontal emittance = 223 μm $\times$ 17.1 μrad $\times$ 0.92 = 3.5 nm·rad

Summary for undulator based e-beam measurements

- The development of the diagnostics undulator beamline has enabled us to measure the beam emittance somewhat independent of beta function.

- Many systematic errors of the undulator-based emittance measurement have been studied theoretically and used to correct the experimental data.

- We developed a new technique for extracting e-beam energy information from undulator spectrum. It has shown good promise to become a high-resolution tool.

- The experiment for energy-dependent e-beam property measurement has illustrated the power of the undulator as a diagnostics device.

- The diagnostics undulator beamline has been instrumental in our exploration of a new operating regime of low beam emittance. One can comfortably use the data taken at this beamline to predict the performance of user ID beamlines in the low-emittance regime.

Undulator beamline upgrade

- The procurement of a cryogenically cooled monochromator is in progress. It will improve the resolution of divergence measurements with the use of the undulator third harmonic, and improve the temporal resolution of the measurement with the increased photon flux.

IV. Summary and Future Development

- Our basic photon monitor, the x-ray pinhole camera at 35-BM has matured with the storage ring: Its stability and resolution are compatible with the current user requirements.

- Many time-resolved imaging techniques, using streak and gated cameras, have been made available to machine studies and have become critical tools for characterizing accelerator beam dynamics.

- The undulator-based beam diagnostics have gone through a rapid development process in FY1999. We expect further development in FY2000.

- Continued vigorous research and development efforts in x ray-based diagnostics are needed for the future needs of this light source and the next generation of light sources.